4th Intercontinental Geoinformation Days

igd.mersin.edu.tr

Geostatistical-based mapping of topsoil texture in Fluvisols and Vertisols around Lake of Manyas

Fuat Kaya*[1], Onur Meşe [1], Levent Başayiğit [1]

[1]*Isparta University of Applied Sciences, Department of Soil Science and Plant Nutrition, Isparta, Türkiye*

Keywords
Geostatistics
Soil particle fractions
Manyas
Kriging
IDW

Abstract

It is critical to understand the spatial distribution of soil particle fractions to create sustainable soil management methods. The spatial distribution of particle fractions has long been studied using geostatistics. Soil particle fractions can be assessed and mapped using a variety of approaches, but selecting the best appropriate method for anywhere has always been a controversial topic in all soil mapping applications. In this study, there is an evaluation of the estimation performance of ordinary kriging (OK) and IDW (Inverse distance weighting) methods for digital mapping of soil particle fractions. It was determined that the clay content of the soil samples was between 24% and 76%, the sand content was between 2% and 69%, and the silt content was between 3% and 44%. The performance of the models was evaluated by the results of the root mean square error (RMSE) and the sum of the fractions. The best results were found using the OK method for Silt (RMSE: 5.36%), while IDW produced more high predictions for Clay (RMSE: 13.80%) and Sand (RMSE: 19.90%). In the control of composition structure, IDW is the method that most closely predicted the relative sum of the three fractions defined as 100%. Creating texture classes in a GIS environment and comparing the efficiency of the produced soil fraction maps is advised.

1. Introduction

The relative proportions of sand, silt, and clay are key soil properties that affect many important physical, chemical, and biological properties of soils (Saurette et al., 2022). Each particle fraction's geographic variation patterns are critical for the creation of sustainable management techniques.

Besides the inverse distance weighting (IDW) method, which is based on Tobler's first law of geography and has no additional requirements regarding spatial distribution and sample size (Zhu et al., 2018), ordinary kriging (OK), a linear geostatistical interpolation technique based on weighting the sums of values at adjacent sampled points are the most widely used spatial modeling applications for the estimation of soil particle fractions (Mousavi et al., 2017).

From fluvial (river terraces) and colluvial sediments to marine and lacustrine deposits containing marl, shale, claystone, and flysch as well as limestone and basalts, Turkiye's vertisols have a wide range of parent materials. Moreover, these soils are also in spatial proximity to Fluvisols, which are predominantly formed in aquatic sediments associated with rivers and flood plains, and lake (Özsoy and Aksoy, 2007). The delta of the Kocaçay River and the lacustrine deposits of Lake Manyas form the Fluvisol-Vertisol landscape in our study area.

Any particular area's soil particle fractions are controlled by geological and pedological factors, which affect their spatial variability. However, in locations where alluvial processes are in play, this variability can be extremely large.

Soil texture is one of the most well-known types of compositional data. Soil particle fractions that are relevant to our investigation total 100%. In the process of modeling the soil fractions that we are interested in, this has been a topic that has been overlooked.

The accuracy of this compositional structure can be checked by collecting the raster maps of the obtained clay, silt, and sand fractions in the geographic

* **Corresponding Author**

*(fuatkaya@isparta.edu.tr) ORCID ID 0000-0003-0011-9020
(onur_mese@outlook.com) ORCID ID 0000-0002-8300-8328
(leventbasayigit@isparta.edu.tr) ORCID ID 0000-0003-2431-5763

Cite this study

Kaya, F., Meşe, O., & Başayiğit, L. (2022). Geostatistical-based mapping of topsoil texture in Fluvisols and Vertisols around Lake of Manyas. 4th Intercontinental Geoinformation Days (IGD), 68-73, Tabriz, Iran

information systems environment. Soil scientists can analyze the maps created using this approach in addition to testing the correctness of the model.

This study aims to compare two different geostatistical methods, which have found widespread application in the literature, in an area dominated by fluvisols and vertisols soil types, in terms of surface soil particle fraction.

2. Method

2.1. Study area

Lake of Manyas is in Northwest Türkiye. The research land was located around of lake and covers an undulating area of approximately 600 km2 (N35 Zone UTM, 570000-595000 East, 4440000-4460000 North). The climatic conditions are characterized by an average annual temperature of 15°C and annual precipitation of about 700 mm (TSMS, 2022). From the Precambrian through the Quaternary, the region's geology is divided into distinct strata. It was alluvium transported by rivers that blanketed the area following the Miocene deposition of Neogene limestones and marls (Mater et al., 2003). There are dry agricultural areas in the north of the study area, and extensively irrigated agricultural areas like rice in the south and west, according to CORINE (CLC, 2018). The northern, eastern, and western parts of Lake Manyas are dominated by vertisols, whereas the southern parts are dominated by fluvisols (Aksoy et al., 2010).

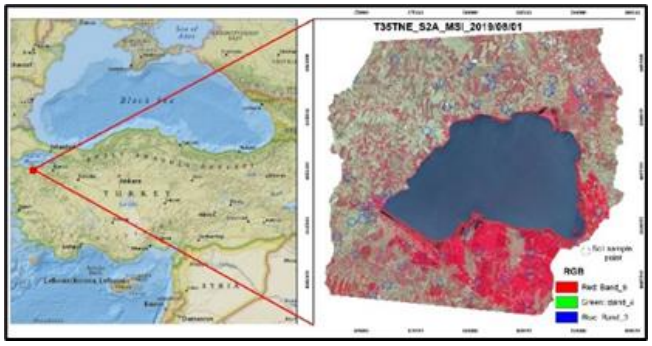

Figure 1. Location of the study area, and the spatial distribution of the soil sampling points overlaid on the Sentinel 2A satellite false-color image

2.2. Soil data

50 soil samples at a depth of 30 cm were taken from the research area between June and August of 2019. The GPS Magellan eXplorist XL was used to record the positions of all sampling points. Fig. 1 depicts the locations of the sampling points. The hydrometer method (Bouyoucos, 1962) was used to determine the distribution of the soil particles fractions were defined based on the international soil particle size classification of sand (0.05 to 2 mm), silt (0.002 to 0.05 mm), and clay (<0.002 mm).

2.3. Geostatistical analysis

Geostatistical analyzes were carried out with the features measured at 50 points of the studied region. Maximum and minimum statistics, mean, standard deviation, skewness, and kurtosis were determined to examine the frequency distribution and determine the descriptive statistics for each fraction (Table 1). Two different geostatistical approaches are presented under separate headings.

2.3.1. Inverse distance weighting (IDW)

The IDW model uses the inverse distance relationship with the following equation to calculate the weights of the values. The IDW interpolation of a value a_j for a given location j is computed as (Emmendorfer and Dimuro 2020):

$$\hat{a}_j^{IDW} = \sum_{i=1}^{n} w_{i,j}\, \hat{a}_i \qquad (1)$$

where each $\hat{a}_i$, i= 1, . . ., n is a data point available at a location i. The weights of $w_{i,j}$, for each data point are given as:

$$w_{i,j} = \frac{d_{i,j}^{-\alpha}}{\sum_{k=1}^{n} d_{i,j}^{-\alpha}} \qquad (2)$$

where $d_{i,j}$, is the Euclidean distance between a data point available at location i and the unknown data at location j; n *is* the number of data points available; α means the power, is a control parameter. The ArcGIS 10.8-Geostatistical Wizard-IDW tool was used to generate distribution maps and model results for geographic coordinated soil particle fractions (ESRI, 2021).

2.3.2. Ordinary Kriging (OK)

To examine the spatial variations of the soil particle fractions, the experimental semivariogram was calculated and the spatial structure of the data was investigated in the studied region. Theoretical models were fitted to these.

The spatial variation structure, the Semivariogram, is determined using the following equation;

$$\gamma(h) = \frac{1}{2n(h)} \sum_{n=1}^{n} [Z(X_i) - Z(X_i + h)]^2 \qquad (3)$$

where n is the number of pairs of the sample separated by the distance h and $Z_{(Xi)}$ the value of sampled point in ith point *(i = 1,2,3, ..., n)*. Each of the three fractions studied had a different best model (in terms of RMSE) (Fig. 2, Table 3).

To estimate soil particle fraction at unsampled points

$$Z(\mu) = \sum_{i=1}^{n} \lambda_i Z(\mu_i) \qquad (4)$$

where $Z_{(\mu)}$ is the predicted value of unsampled point; $Z_{(\mu i)}$ is the i_{th} point by measured value; λ_i is the ith point by undefined weight for the estimated value; n is the number of sampled values.

The ArcGIS 10.8-Geostatistical Wizard-Ordinary Kriging tool was used to generate distribution maps and model results for geographic coordinated soil particle fractions (ESRI, 2021).

2.4. Summation of the predicted soil particle size fractions

Clay, silt, and sand all make up 100% of the soil texture composition. Using such data, the predicted components must amount to 100% over the entire model (Amirian-Chakan et al., 2019). Raster maps of the soil particle fraction produced by two different approaches were collected with the ArcGIS 10.8-Arctoolbox-Spatial Analyst-Map Algebra-Raster calculator tool (ESRI, 2021).

3. Results

3.1. Descriptive statistics of soil particle fractions

Table 1 was listed the descriptive statistics results of the analyzed datasets. In the study area, the highest average was determined in Clay with 48.2%, while the lowest was in Silt with 19.8%.

Table 1. Descriptive statistics of soil particle fractions. Abbreviations: SD: Standard deviation, CV: Coefficient of Variation (%). Min.: Minimum, Max.: Maximum, Ske.: Skewness, Kur.: Kurtosis

	Mean	SD	CV	Min.	Max.	Ske.	Kur.
Clay	48.2	13.2	27.4	24.1	75.6	0.0	-0.9
Silt	19.8	6.7	33.8	3.00	44.2	1.5	5.0
Sand	31.9	13.5	42.4	2.60	68.6	0.3	0.0

The highest coefficient of variation (CV) in the study area was found in the sand with 42.4%. The skewness coefficients were quite close to 0 for clay and sand, while positive skewness values were present for Silt. Meanwhile, the kurtosis coefficient for silt was quite high compared to the other two fractions (Table 1).

3.2. Variogram analysis and spatial autocorrelation

Figure 2 depicts the experimental variograms of clay, silt, and sand content, together with the fitted different models.

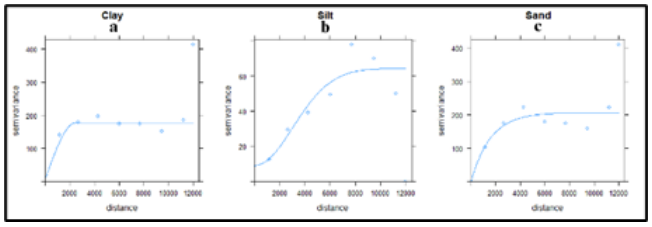

Figure 2. Variograms and fitted models.

The tested models (Spherical, Gaussian, Exponential) were modeled with an experimental variogram of soil fractions. The nugget: sill ratio (NSR) represents a contribution of the nugget to the overall spatial structure of the variogram and it can be calculated as NSR = $C_0/(C_0+C)$. The NSR indicates how geographically dependent or autocorrelated the measured attribute is. Ratios below 0.25 indicate a strong spatial correlation, while ratios above 0.75 indicate a weak spatial correlation, with a median value between 0.25 and 0.75 suggesting moderate spatial dependency (Adhikari et al. 2013). The NSR ranged from 0.0 to 0.12 within the three fractions, showing strong spatial dependence (Table 2).

Table 2. Semivariogram model properties for soil particle fractions.

Soil particle fractions	Model	Nugget (c_0)	Sill (c_0+c)	Nugget /Sill Ratio	Range (m)
Clay	Sph.	8.74	177.2	0.04	2425
Silt	Gau.	6.48	51.9	0.12	5450
Sand	Exp.	0.0	188.9	0.0	3358

3.3. Model performance and predicted maps

Table 3 displays the results of modeling soil particle fractions with IDW and OK geostatistical methods. The fitted variograms for the soil particle fractions were spherical for Clay, gaussian for silt, and exponential for sand (Fig. 2 and Tablo 3). Zeraatpisheh et al. (2022) found predominantly spherical and exponential mathematical models in the modeling process of soil fractions. While for Silt the lowest root mean square error values were obtained from the OK-Gaussian model, Clay and Sand, it was obtained from the model produced as a result of setting the power parameter of IDW to 1 (Table 3).

Table 3. Comparisons of the accuracy of IDW and OK models for cross-validation results of soil particle fractions (Root mean square value)

Fractions	OK			IDW	
Model /Parameter	Sph.	Exp.	Gau.	1	2
Clay	14.47	14.54	14.63	13.80	14.68
Silt	5.54	5.71	5.36	6.16	6.06
Sand	14.54	14.31	14.37	13.94	14.54

Continuous maps for each soil fraction in the study area were shown in Fig. 3. Both different methods produced similar distributions for clay and silt. The southeast of the study area was characterized by higher silt and lower sand contents than the overall area (Fig. 3-a-d). This was a considerable difference in the distribution of the sand fraction between the two models. Considering the minimum and maximum values in the data set for Sand (Table 1), it is seen that the OK method cannot exemplify the minimum values of Sand (Fig.4-f).

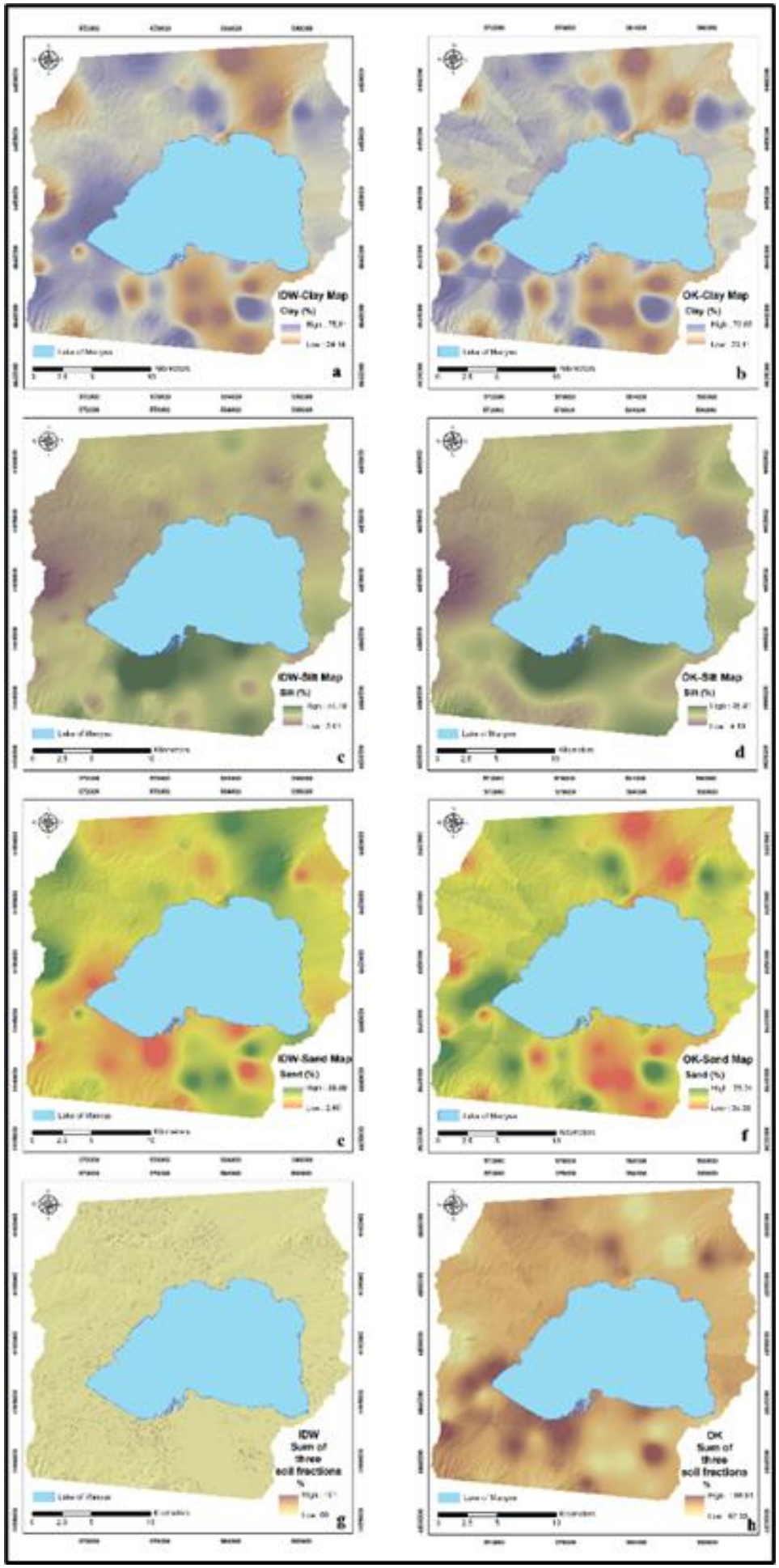

Figure 3. Map of predicted soil particle fractions

4. Discussion

Spatial modeling of each of the soil particle fractions is a popular approach because of the particular importance of each of the fractions (Saurette et al., 2022). Geostatistical models based on distinct mathematical foundations shows to have similar model accuracy (Table 3). Significant differences were determined for Sand in particular for the produced spatial maps. Here, it should be well known for IDW that the maximum and minimum of estimated values from IDW are limited to the extreme data points in the data set (Emmendorfer and Dimuro, 2020). When compared to OK, this IDW made no significant change in forecast maps for Silt and Clay, while it made a substantial difference for Sand. IDW was found to be more successful in reflecting the minimum and maximum values of the sand fraction better in the fluvisols areas concentrated in the southeast of the study area. OK and IDW produced similar distribution maps and minimum and maximum values for silt. Again for Clay, OK and IDW produced similar minimum and maximum values, while OK produced sharp map boundaries. (Fig. 3-b,f). The sharp boundaries that OK produces based on mathematical calculations may not have a counterpart in the field. The fact that OK produces such maps, especially for Sand and Clay, may be related to the decrease in model accuracy values (Table 3). Sharply demarcated maps may not represent the mapping unit boundary approach in soil maps. Soil texture, which is well-known for its compositional structure, must be evaluated to see if these three functions are all equal to 100% totally. Considering the maps produced as a result of collecting the estimated 3 fractions in a raster environment, those regions that have a total of more than 100 and less than 100 are concentrated in the research area's southern and southeasterly sections (Fig. 3-h). These regions are characterized by alluvial deposits. In this regard, it is recommended to carry out spatial mapping applications by making precise and more sampling in these regions, specific to the study area. High changes in soil fraction at short distances are characteristic of alluvial deposition zones (Basayigit and Senol, 2008). Similarly, in a study area that developed mainly on Quaternary aged alluvial deposits, the totals of the spatially estimated soil fraction maps with different approaches appeared in the range of 96% to 104 (Amirian-Chakan et al., 2019). The summing values for IDW range from 99 to 101%, whereas the summing values for OK range from 62.39 to 166.91% based on our findings (Fig. 3 g-h). The mathematical basis of the OK method for each fraction may have caused this difference. Using GIS tools, it is possible to create texture classes and compare the resulting soil particle fractions (Saurette et al., 2022).

3. Conclusion

The results of our study demonstrate the effectiveness of 2 different well-known geostatistics (OK and IDW) applications to study and analyze the spatial behavior of soil texture content in an area with high variability over short distances. To evaluate the uncertainty of the maps obtained, the collection of the fractions we suggest and the control due to the compositional structure should be expressed as a significant issue. For soil surveyors, the geostatistical-based model must resemble natural classes that will form the distribution map of soil texture, as well as statistical success. Using other data layers such as digital data to represent the formation of soils (topographic parameters, parent material, organism) and other information that may affect the spatial distribution of soil texture in fluvisols and vertisols, and using advanced statistical learning algorithms suggest that studies be carried out by making more analysis in a way that can reveal non-linear relationships.

References

Adhikari, K., Kheir, R. B., Greve, M. B., Greve, M. H. (2013). Comparing kriging and regression approaches for mapping soil clay content in a diverse Danish landscape. Soil science, 178(9), 505-517. https://doi.org/10.1097/SS.0000000000000013

Aksoy, E., Panagos, P., Montanarella, L., Jones, A. (2010). Integration of the soil database of Turkey into European soil database 1: 1.000. 000. European Commission JRC Research Report, EUR 24295EN. Italy.

Amirian-Chakan, A., Minasny, B., Taghizadeh-Mehrjardi, R., Akbarifazli, R., Darvishpasand, Z., Khordehbin, S. (2019). Some practical aspects of predicting texture data in digital soil mapping. Soil and Tillage Research, 194,104289.https://doi.org/10.1016/j.still.2019.06.0060.1016/j.still.2019.06.006

Basayigit, L., Senol, S. (2008): Comparison of soil maps with different scales and details belonging to the same area. Soil and Water Research, 3, 31-39.

Bouyoucos, G. J. (1962). Hydrometer method improved for making particle size analyses of soils. Agronomy Journal, 54,464-465. https://doi.org/10.2134/agronj1962.00021962005400050028x

CLC (2018). Corine land cover class 2018 V 2.0 data. (Accessed 04 October 2021).

Emmendorfer, L. R., & Dimuro, G. P. (2020). A Novel Formulation for Inverse Distance Weighting from Weighted Linear Regression. Lecture Notes in Computer Science. Springer, Cham. https://doi.org/10.1007/978-3-030-50417-5_43

ESRI, (2021). ArcGIS user's guide, http://www.esri.com.

Mater, B., Turoğlu, H., Uludağ, M., Cürebal, İ., Yıldırım, C. (2003). Uluabat-Manyas Gölleri ve Yakın Çevresinin Jeomorfolojik Gelişim Modellemesi. Türkiye Kuvaterneri Çalıştayı IV, 180-186, Türkiye.

Mousavi, S. R., Sarmadian, F., Dehghani, S., Sadikhani, M. R., Taati, A. (2017). Evaluating inverse distance weighting and kriging methods in estimation of some physical and chemical properties of soil in Qazvin Plain. Eurasian Journal of Soil Science, 6(4), 327-336. https://doi.org/10.18393/ejss.311210

Özsoy, G., Aksoy, E. (2007). Characterization, classification and agricultural usage of vertisols developed on neogen aged calcareous marl parent materials. Journal of Biological & Environmental Sciences, 1(1), 5-10.

Saurette, D. D. (2022). Comparing direct and indirect approaches to predicting soil texture class. Canadian Journal of Soil Science, https://doi.org/10.1139/CJSS-2022-0040

TSMS (2022). Turkish State Meteorological Service.

Zeraatpisheh, M., Bottega, E. L., Bakhshandeh, E., Owliaie, H. R., Taghizadeh-Mehrjardi, R., Kerry, R., & Xu, M. (2022). Spatial variability of soil quality within management zones: Homogeneity and purity of delineated zones. CATENA, 209, 105835. https://doi.org/10.1016/j.catena.2021.105835

Zhu, A., Lu, G., Liu, J., Qin, C., & Zhou, C. (2018). Spatial prediction based on Third Law of Geography. Annals of GIS, 24(4), 225–240. https://doi.org/10.1080/19475683.2018.1534890